

Measurements of quasiparticle thermalization in a normal metal

J. N. Ullom,^{*} P. A. Fisher,[†] and M. Nahum,[‡]

Department of Physics, Harvard University, Cambridge, Massachusetts 02138

(Received 15 July 1999)

We have probed the inelastic relaxation of gap-edge quasiparticles in a superconductor to conduction electrons in an adjoining normal metal. Quasiparticles are injected into a superconducting Al film by a normal-insulator-superconductor tunnel junction at a temperature of about 100 mK. These quasiparticles diffuse throughout the superconductor and those that do not recombine are trapped in an adjoining Ag film. We find that trapped quasiparticles transfer more than 80% of their excitation energy to conduction electrons in the Ag over a broad range of electron and phonon temperatures and explain this result with a model that incorporates electron-electron, electron-phonon, and phonon-electron interactions.

The manner by which excited electrons relax in a metal depends strongly on the initial electron energies and on the relative rates for electron-electron and electron-phonon interactions. A technologically important range of excitation energies occurs near 1 meV, when gap-edge quasiparticles from a low-temperature superconductor diffuse into an adjoining metal. This phenomenon arises in a class of cryogenic detectors first proposed by Booth which use a large-area superconducting absorber to convert incident quanta into quasiparticle excitations and an adjoining superconductor with lower energy gap to spatially confine, or “trap,” quasiparticles that enter and scatter inelastically.¹ A sensitive measurement of the number of quasiparticles is then performed. Quasiparticle trapping in a superconductor has been studied extensively and is used in superconducting tunnel junction detectors for applications including single-photon counting at optical wavelengths and high resolution x-ray spectroscopy.^{2–4} Quasiparticle trapping in a normal metal was first suggested and used for weakly interacting dark matter detectors⁵ and appears to offer substantial benefits when integrated with thermal sensors that measure the energy deposited in the normal trap with great accuracy.^{6,7} A normal-metal quasiparticle trap is the basis for a recently proposed superconducting three-terminal device⁸ and normal metal traps can greatly improve the performance of normal-insulator-superconductor tunnel junction refrigerators.^{9,10} In light of this body of work, it is useful to investigate in detail the nature of quasiparticle relaxation in a normal metal.

We report measurements of the relaxation of quasiparticles from superconducting aluminum to the Fermi sea in normal silver. We find that quasiparticles which relax in the normal-metal transfer over 80% of their excitation energy to conduction electrons, and that this fraction changes only slightly for electron temperatures in the metal over the range 85–380 mK and for phonon temperatures over the range 100–250 mK. In what follows, we first describe our device and measurement technique. We then deduce the average energy a trapped quasiparticle transfers to the Fermi sea and show that it is largely independent of the electron and phonon temperatures in the trap. We explain these results with a model that describes the relaxation of excited electrons in a normal metal. This model incorporates new calculations of the electron-phonon and phonon-electron scattering rates for

individual electrons and phonons. Finally, we use our quasiparticle relaxation model to make predictions about trapping from larger gap superconductors at higher temperatures.

An energy-level diagram of our device is shown in Fig. 1. Current flow through a normal-insulator-superconductor (NIS) tunnel junction injects quasiparticles into the superconducting electrode. While some quasiparticles recombine in the superconductor, a measurable fraction diffuse into a normal film which makes metallic contact to the superconductor. Quasiparticles that enter the metal and scatter inelastically are trapped, and subsequently thermalize to the Fermi sea via electron-electron and electron-phonon interactions. The ratio of the energy transferred to the electron system and the quasiparticle excitation energy is hereafter referred to as the thermalization efficiency. For device applications, a thermalization efficiency near unity is desirable.

A schematic of the device is shown in Fig. 2. Quasiparticles are injected into the central superconducting Al film by one of two NIS tunnel junctions. The quasiparticle trap is the

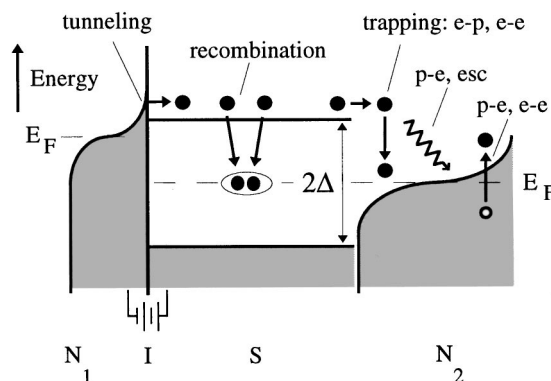


FIG. 1. Energy-level diagram. Occupied states are shaded. NIS junction electrodes are marked $N1$ and S . Current flow through the junction creates quasiparticles in S . Some quasiparticles recombine before reaching an adjacent normal metal film marked $N2$. Quasiparticles which scatter inelastically in $N2$ are trapped. Quasiparticles relax in $N2$ by electron-phonon ($e-p$) and electron-electron ($e-e$) interactions. A phonon (jagged line) emitted by a relaxing quasiparticle can interact with other electrons ($p-e$) or escape the trap (esc). Electrons in the trap are heated by phonon-electron ($p-e$) and electron-electron ($e-e$) interactions.

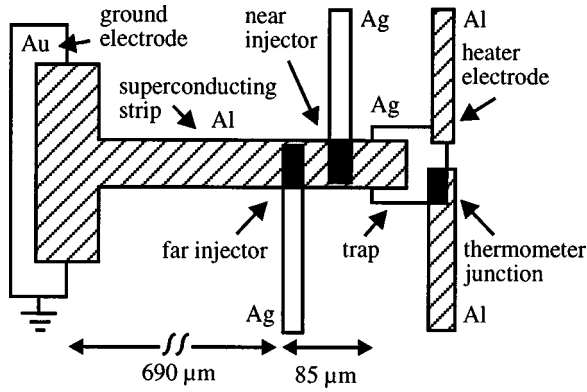


FIG. 2. Device schematic: superconducting films are cross-hatched, normal films are clear, tunnel junction regions are dark. Two NIS junctions, labeled near and far, are used to inject quasiparticles into a 75 nm thick Al strip. The Al had a resistivity of $5.6 \mu\Omega \text{ cm}$ at 4.2 K and a calculated normal-state diffusion constant $D_n = 53 \text{ cm}^2/\text{s}$. The thickness of the Ag trap was 140 nm and its resistance was measured to be $0.040 \pm 0.004 \Omega$. This uncertainty implies a systematic error in our measurements of P_d of less than 10%. Not shown are additional superconducting films used to make a four-point resistance measurement of the trap and also to reduce Joule heating in the normal electrodes of the injector junctions. All features to the right of the far injector are to scale with the $85 \mu\text{m}$ arrow. Features to the left of the far injector are not to scale. The superconducting strip broadens to make good electrical contact with the ground electrode. The broadening is sufficiently distant ($370 \mu\text{m}$) from the far injector that the diffusion of quasiparticles takes places almost entirely in the narrow region. The device was fabricated in a single vacuum cycle using thermal and electron beam evaporation through a micromachined Si mask and was cooled in a magnetically shielded environment.

Ag film which makes metallic contact to the Al. The temperature of electrons in the Ag is measured from the current-voltage characteristics of a third NIS junction, where part of the Ag forms the normal electrode. An additional superconducting electrode makes metallic contact to the Ag. Current flow through this heater electrode dissipates a known Joule power directly and entirely into the electron system and thus provides a calibration for the response of the thermometer junction to deposited power. The thermometer response is also calibrated directly against temperature by warming the substrate, thereby heating both electrons and phonons throughout the device. The circuit ground is positioned sufficiently far from the injector junctions so that a negligible fraction of the injected quasiparticles diffuse into the ground electrode.

A typical measurement consists of the steady-state injection and detection of quasiparticles. A current I is passed through one of two injector junctions thus creating quasiparticles in the central Al strip at a rate (I/e) . The power injected into the superconductor P_i is $(I/e)\langle E \rangle$, where $\langle E \rangle$, the average injected quasiparticle energy, is calculated from the voltage, V , across the junction and the electron temperature T_e in the electrodes via the relation

$$\langle E \rangle = \frac{\int_{\Delta}^{\infty} EK(E, V, T_e) dE}{\int_{\Delta}^{\infty} K(E, V, T_e) dE}. \quad (1)$$

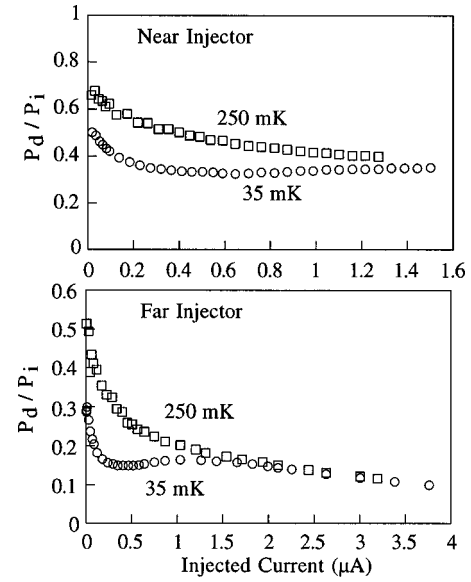


FIG. 3. Dependence of P_d/P_i on current injected through the near and far junctions at substrate temperatures of 35 and 250 mK. At 35 mK, the currents corresponding to injector voltages of Δ/e and $1.1\Delta/e$ are 0.3 and 1.0 μA , respectively, for both junctions.

Here $K(E, V, T_e) = E(E^2 - \Delta^2)^{-1/2} [f(E + eV, T_e) + f(E - eV, T_e) - 2f(E, T_e)]$, $f(E, T_e)$ is the Fermi function, and Δ is the superconducting gap energy. We calculate that self-heating in the injector junctions can increase T_e slightly above the phonon temperature and include this effect when deducing $\langle E \rangle$. For our experimental conditions, $\langle E \rangle$ is typically within 10% of Δ . We measure the power P_d that quasiparticles deposit in the Fermi sea of the trap by finding the applied Joule power that yields the same rise in trap temperature as the injected current I .¹¹ In the absence of recombination, all the quasiparticles reach the trap and therefore the ratio P_d/P_i is equal to the thermalization efficiency.¹² In the presence of recombination P_d/P_i forms a lower bound. We use data from injection at two distances from the trap to quantify and correct for the effects of recombination.

In Fig. 3 we show the measured dependence of P_d/P_i on injected current at substrate temperatures of 35 and 250 mK for both injector junctions. As explained in Ref. 13, the ratio P_d/P_i decreases with current due to recombination within the injected population. Furthermore, P_d/P_i increases when the substrate temperature is raised because the quasiparticle velocity is a strongly increasing function of injection energy $\langle E \rangle$ for energies near Δ and $\langle E \rangle$ is an increasing function of the electron temperature in the injector. Consequently, quasiparticles diffuse more rapidly at elevated temperatures, and recombination is reduced. Therefore, the least recombination occurs in the low-current, high-temperature data for the near junction and P_d/P_i in this regime is closest to the thermalization efficiency. This lower bound is 65%. It is evident, however, that recombination losses are still present because P_d/P_i from the far injector is lower than P_d/P_i for the near at low currents. To estimate P_d/P_i in the absence of recombination we measure P_d/P_i from injection at two distances from the trap. We use a linear fit between the two injector locations to estimate P_d/P_i due to injection at the Al/Ag interface and deduce a thermalization efficiency of at least 80%.¹³

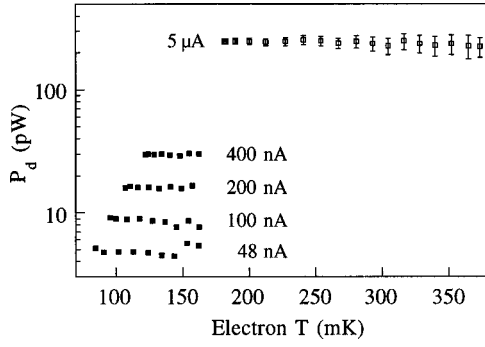


FIG. 4. Dependence of the deposited power P_d on electron temperature in the trap for five injection currents. Open squares denote data taken in a second device. For clarity, error bars are shown only for this data set. Note that the error increases with temperature. Temperatures below 100 mK may be underestimated due to self-heating by the thermometer. The substrate temperature is 35 mK.

By dissipating Joule power in the trap during quasiparticle injection, we are able to probe the dependence of the thermalization efficiency on electron temperature in the trap. In Fig. 4 we show the dependence of P_d on electron temperature for four different currents through the near injector. Also shown is data from a second sample for a higher injection current and a larger temperature range. We find that P_d is independent of electron temperature from 85 to 165 mK and is reduced by about 8% between 180 and 380 mK. We deduce that the relaxation of electrons with $\langle E \rangle \approx \Delta$ in a normal metal is only weakly dependent on the temperature of the Fermi sea. This is a reasonable conclusion since Δ is many times larger than thermal excitation energies in the metal. For our Al, Δ/k_b is 2.56 K and the electron temperatures, T_e , encountered in the normal Ag trap are less than 380 mK.

We are also able to probe the dependence of the thermalization efficiency on the phonon temperature in the trap by varying the substrate temperature and hence the temperature of both electrons and phonons throughout the device. Since the electron temperature in the trap does not affect the thermalization efficiency, warming the substrate tests for a dependence on phonon temperature. However, as previously discussed, quasiparticle recombination in the Al strip is also dependent on temperature, thus potentially masking any temperature effects in the trap. To separate these two effects, we consider the response of the trap to injection only at voltages somewhat above Δ/e , where $\langle E \rangle$, and thus recombination, are essentially independent of temperature. These voltages correspond to currents greater than $1.75 \mu\text{A}$ in our device. It can be seen in Fig. 3 that P_d/P_i is independent of substrate temperature at these currents over the range 35–250 mK. At these high currents, we calculate that power flowing from the electrons produces some heating of the phonons in the trap. The range of phonon temperatures probed is believed to be from roughly 100 to 250 mK. We thus conclude that the average energy a trapped quasiparticle transfers to the Fermi sea is independent of phonon temperature in the trap over this range.

To understand this near-perfect thermalization over a broad range of electron and phonon temperatures, we have developed a model that describes the relaxation of excited electrons in a normal metal film. A hot electron relaxes by electron-electron and electron-phonon interactions which

produce lower-energy electronic excitations and phonons. Energy is lost from the trap when these phonons escape into the substrate before interacting with other electrons. We model the relaxation process by solving the following coupled differential equations for the time-varying electron and phonon densities in the trap $n(E)$ and $N(E)$, respectively, at discrete energy levels E :

$$\begin{aligned} \frac{dn(E)}{dt} = & -\frac{n(E)}{\tau_{e-e}(E)} - \frac{n(E)}{\tau_{e-p}(E)} + \frac{3n(3E)}{\tau_{e-e}(3E)} + \frac{n(4E)}{\tau_{e-p}(4E)} \\ & + \frac{2N(2E)}{\tau_{p-e}(2E)}, \end{aligned} \quad (2)$$

$$\frac{dN(E)}{dt} = +\frac{n(4E/3)}{\tau_{e-p}(4E/3)} - \frac{N(E)}{\tau_{p-e}(E)} - \frac{N(E)}{\tau_{\text{esc}}}. \quad (3)$$

The first and second terms on the right side of Eq. (2) describe the relaxation of electrons to lower energy states by electron-electron and electron-phonon interactions at energy-dependent rates $1/\tau_{e-e}(E)$ and $1/\tau_{e-p}(E)$, respectively. The third and fourth terms in Eq. (2) describe the population of energy level E by electrons relaxing from higher energy states. The fifth term in Eq. (2) describes the population of energy level E by electrons excited from the Fermi sea by phonon absorption, where $1/\tau_{p-e}(E)$ is the phonon-electron interaction rate for a phonon of energy E . Numerical factors multiplying E in Eq. (2) arise from calculations of the average energy exchanged in each scattering process. We calculate that, on average, electron-electron and electron-phonon processes reduce the energy of the relaxing electron by factors of 3 and 4, respectively, and that phonon-electron processes produce excitations with half the energy of the absorbed phonon. These results are derived in the limit $E \gg k_b T_e$ but are also applied to lower energies. Numerical factors multiplying n and N in Eq. (2) describe the number of excitations created by each scattering process. Electron-electron and phonon-electron processes produce 3 (2 electrons and 1 hole) and 2 (1 electron and 1 hole) excitations, respectively. In Eq. (3), the first term on the right describes the creation of phonons by electron-phonon processes. The factor of $4/3$ occurs because, as described earlier, phonons of energy E are emitted by electrons with energy $4E/3$. The second term describes the loss of phonons due to absorption by electrons, and the third describes the loss of phonons to the substrate at an energy-independent rate $1/\tau_{\text{esc}}$. We assume that only electrons from the Fermi sea are excited to higher states, that all interactions occur with the average energies outlined above, and that holes relax in the same manner as electrons. Electrons are considered thermalized when they reach energies below $E = k_b T_e$.

We next estimate the scattering times in Eqs. (2) and (3). Because of the strong dependence of the electron-phonon scattering time on electron energy, it is important to use the scattering time for a single electron with the energy of interest rather than the characteristic scattering time in a thermal distribution. We derive the electron-phonon scattering time for single excited electrons $\tau_{e-p}(E)$ from the deformation potential approximation described in Ref. 14. We calculate that

$$\tau_{e-p}(E) = 3I_0 D(E_f) k_b^5 / (\Sigma E^3), \quad (4)$$

where E is the excitation energy of the electron relative to the Fermi level and both the electrons and phonons in the trap are at 0 K.¹⁵ The factor I_0 is $\Gamma(5)\zeta(5) \approx 25$, $D(E_f)$ is the electronic density of states at the Fermi level, and Σ is the electron-phonon coupling constant. The deformation potential treatment predicts that if the electrons and phonons in a metal are at well defined but different temperatures T_e and T_p , respectively, the power flow between them is given by $\Sigma U(T_e^5 - T_p^5)$ where U is the volume of the metal.¹⁴ Using the heater electrode to dissipate a known Joule power in the electrons of the trap, and the thermometer junction to measure their temperature rise, we find an excellent fit to this functional dependence when Σ equals 2.1 nW/(K⁵ μm^3). Again in the deformation-potential approximation, we calculate that the phonon-electron scattering time is

$$\tau_{p-e}(E) = I_0 D(E_f) k_b^5 / (2\Sigma m^2 s^3 v_f E), \quad (5)$$

where E is the phonon energy and the Fermi sea is at 0 K. Here, m is the electronic mass, v_f is the Fermi velocity, and s is the longitudinal phonon velocity. (Only longitudinal phonons contribute to the electron-phonon coupling in Ref. 14.) More detailed calculations of $\tau_{e-p}(E)$ and $\tau_{p-e}(E)$ that include the effects of finite temperature have been performed; however, it is reasonable to simply substitute $E + k_b T_e$ for E . The phonon temperature affects relaxation only through stimulated emission and can be ignored in the temperature regime that we have explored since the average occupancy of phonon energy levels is considerably smaller than unity.¹⁵

The phonon escape time τ_{esc} depends on the phonon transmission probability η at the film-substrate interface and the attempt frequency on the interface. We take τ_{esc} equal to $4d/(\eta s)$ where d is thickness of the trap.¹⁶

The electron-electron scattering time $\tau_{e-e}(E)$ for an excitation of energy E is the least well-known of the scattering times. We adapt calculations given in the literature for the characteristic scattering time in an electron distribution at temperature T_e to the case of a single excitation by substituting E/k_b for T_e . Based on the film thickness and mean free path, we estimate that the silver trap appears two-dimensional (2D) and clean to an excitation with $E = \Delta$.¹⁵ In this regime,¹⁷

$$\tau_{e-e}(E) = 2\hbar E_f / [\pi E^2 \ln(E_f/E)]. \quad (6)$$

We also include dirty scattering because the dirty scattering time becomes shorter than the clean time for excitations with E below 0.2 K. In a 2D dirty film

$$\tau_{e-e}(E) = 2\pi\hbar^2 / [q^2 R E \ln(k_b T_1 / E)], \quad (7)$$

where q is the electronic charge, R is the resistance per square of the trap, T_1 is $9 \times 10^5 (k_f l)^3$ K, and l is the electronic mean free path.¹⁸ We add the clean and dirty scattering rates to obtain an effective electron-electron rate and include the effects of finite temperatures by substituting $E + k_b T_e$ for E .

To evaluate the expressions given above, we use $E_f = 5.5$ eV, $D(E_f) = 1.0 \times 10^{29} \text{ J}^{-1} \mu\text{m}^{-3}$, $v_f = 1.4 \times 10^6$ m/s, and $k_f = 1.2 \times 10^{10} \text{ m}^{-1}$.¹⁹ We take $s = 3.8 \times 10^3$ m/s and η

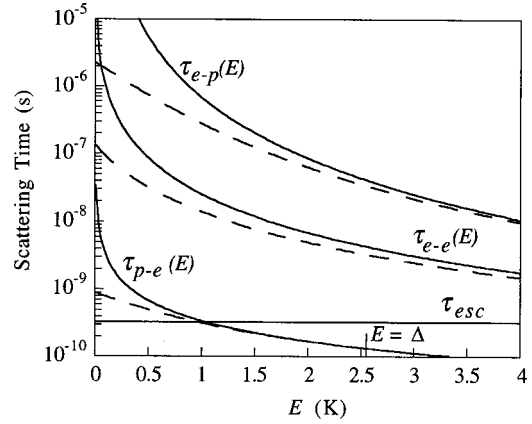


FIG. 5. Calculated electron-phonon, phonon-electron, electron-electron, and phonon escape times in Ag as a function of energy E (measured in degrees K). An excitation which enters the Ag trap from the Al strip has $E \approx 2.56$ K. Solid lines show scattering times for an electron (phonon) temperature in the trap of 0 K (0 K). Dashed lines show scattering times for an electron (phonon) temperature of 380 mK (35 mK). Note that the phonon escape time is independent of phonon energy.

$= 0.45$.^{16,20} Finally, we measure $d = 140$ nm, $l = 150$ nm, and $R = 0.04 \Omega$. When energy E is expressed in Kelvin, we find $\tau_{e-p}(E) = 680/E^3$ ns, $\tau_{p-e}(E) = 0.3/E$ ns, and $\tau_{\text{esc}} = 0.3$ ns. We find $\tau_{e-e}(E)$ to be $30/E^2$ ns in the clean limit and $150/E$ ns in the dirty limit. In Fig. 5, the energy dependencies of all the scattering times are shown for electron (phonon) temperatures of 0 K (0 K) and 380 mK (35 mK).

Equations (2) and (3) predict that an electron elevated by an energy $\Delta = 221 \mu\text{eV}$ above a 170 mK Fermi sphere will transfer 95% of its energy to other electrons as it relaxes, in reasonable agreement with the observed fraction of more than 80%. A thermalization efficiency near unity is a logical consequence of the scattering times in Fig. 5 since the electron-electron scattering time is a factor of 10 shorter than the electron-phonon scattering time for an electron with energy Δ . Of the few phonons emitted, about half return their energy to the electron system because the phonon-electron time for a $3\Delta/4$ phonon is comparable to the phonon escape time. Electron-electron scattering increasingly dominates the thermalization process for lower energy excitations. The predictions of Eqs. (2) and (3) for the thermalization efficiency are relatively robust to changes in the scattering times: increasing $\tau_{e-e}(E)$ by a factor of 5 only reduces the thermalization efficiency to 82%. Furthermore, the model predicts that the thermalization efficiency changes by less than 1% as the electron temperature in the trap rises from 85 to 380 mK. The model shows little sensitivity to electron temperature because the scattering times in Fig. 5 are almost temperature independent for E near Δ .

We have also used the model to probe the dependence of the thermalization efficiency on the choice of superconductor. Trapping from higher gap materials such as Ta and Nb is of particular interest for cryogenic electronics. In Fig. 6 we show the dependence of the calculated thermalization efficiency on the temperature T of the electrons and phonons in the trap for several values of Δ . The trap is Ag as before. The thermalization efficiencies are generally greater than 90% and largely independent of Δ and T . The thermalization ef-

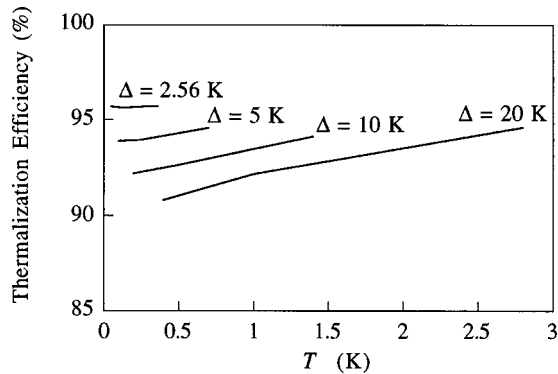


FIG. 6. Calculated thermalization efficiencies as a function of temperature for excitations elevated 2.56, 5, 10, and 20 K above the Fermi surface. The electrons and phonons of the trap are assumed to be in thermal equilibrium.

efficiency remains high for the larger values of Δ where $\tau_{e-p}(\Delta)$ approaches $\tau_{e-e}(\Delta)$ because $\tau_{p-e}(3\Delta/4) \ll \tau_{esc}$. For fixed temperature, the thermalization efficiency falls slightly as Δ increases because higher energy quasiparticles must undergo more relaxation events to reach energies near $k_b T$ and each event is an opportunity for energy to be lost. For fixed Δ , the thermalization efficiency rises slightly with

T because quasiparticles need to undergo fewer relaxation events to be considered thermalized.

In conclusion, we have measured that the electrons in an Ag film absorb more than 80% of the energy of quasiparticles trapped from an adjoining Al film over a wide range of electron and phonon temperatures. We explain this result with a calculation that describes the relaxation of hot electrons in a normal metal by electron-electron, electron-phonon, and phonon-electron processes. We have extended this calculation to superconductors with larger energy gaps than Al and predict that the thermalization efficiency remains close to unity. Our experimental and theoretical results suggest that normal metal traps are a useful means of concentrating quasiparticle energy in superconducting electronics.

This work was supported by the CFPA Program of the NSF under Grant No. SA1306-22311NM, by NASA under Grant No. NGT-51405, and in part by the MRSEC Program of the NSF. J.N.U. was supported by NASA GSRP. This work was also performed under the auspices of the U.S. Department of Energy by University of California Lawrence Livermore National Laboratory under Contract No. W-7405-Eng-48. We thank J. A. Oswald and E. Abrahams for valuable discussions and C. A. Mears for a critical reading of the manuscript.

*Present address: Lawrence Livermore National Laboratory, PO 808, L418, Livermore, CA 94550.

†Present address: Analog Devices Corporation, 804 Woburn, MS-426, Wilmington, MA 01887.

‡Present address: MicroEncoder Inc., 11533 N.E. 118th Street, Kirkland, WA 98034.

¹N. E. Booth, Appl. Phys. Lett. **50**, 293 (1987).

²H. Kraus, F. von Feilitzsch, J. Jochum, R. L. Mossbauer, T. Peterreins, and F. Probst, Phys. Lett. B **231**, 195 (1989).

³A. Peacock, P. Verhoeve, N. Rando, A. van Dordrecht, B. G. Taylor, C. Erd, M. A. C. Perryman, R. Venn, J. Howlett, D. J. Goldie, J. Lumley, and M. Wallis, Nature (London) **381**, 135 (1996).

⁴C. A. Mears, S. E. Labov, M. Frank, and M. A. Lindeman, Nucl. Instrum. Methods Phys. Res. A **370**, 53 (1996).

⁵K. D. Irwin, S. W. Nam, B. Cabrera, B. Chugg, and B. A. Young, Rev. Sci. Instrum. **66**, 5322 (1995), and references therein.

⁶K. D. Irwin, G. C. Hilton, D. A. Wollman, and J. M. Martinis, Appl. Phys. Lett. **69**, 1945 (1996).

⁷M. Nahum and J. M. Martinis, Appl. Phys. Lett. **66**, 3203 (1995).

⁸N. E. Booth, P. A. Fisher, M. Nahum, and J. N. Ullom, Supercond. Sci. Technol. **12**, 538 (1999).

⁹J. N. Ullom and P. A. Fisher, Physica B (to be published).

¹⁰J. P. Pekola *et al.* (unpublished).

¹¹We have measured the thermal response of the trap in similar devices when the interface between the Al strip and the Ag trap was physically scratched and found that heating through the substrate is present but negligible compared to heating by quasiparticles when the interface is intact.

¹²The energy lost due to quasiparticles emitting phonons and relaxing to lower energy states in the superconductor is negligible because the inelastic scattering time is long compared to the diffusion time to the trap for $\langle E \rangle \approx \Delta$. See Ref. 13, and references therein.

¹³J. N. Ullom, P. A. Fisher, and M. Nahum, Phys. Rev. B **58**, 8225 (1998).

¹⁴F. C. Wellstood, Ph.D. thesis, University of California, Berkeley, 1988.

¹⁵J. N. Ullom, Ph.D. thesis, Harvard University, 1999.

¹⁶S. B. Kaplan, J. Low Temp. Phys. **37**, 343 (1979).

¹⁷H. Fukuyama and E. Abrahams, Phys. Rev. B **27**, 5976 (1983).

¹⁸P. Santhanam and D. E. Prober, Phys. Rev. B **29**, 3733 (1984).

¹⁹C. Kittel, *Introduction to Solid State Physics*, 6th ed. (Wiley, New York, 1986).

²⁰E. T. Swartz and R. O. Pohl, Rev. Mod. Phys. **61**, 605 (1989).